On the relation between unimolecular reaction rates and overlapping resonances

Uri Peskin, Hanna Reisler,[a] and William H. Miller
Department of Chemistry, University of California, and Chemical Sciences Division, Lawrence Berkeley Laboratory, Berkeley, California 94720

(Received 19 July 1994; accepted 25 August 1994)

Unimolecular decay processes are studied in the regime of overlapping resonances with the goal of elucidating how unimolecular reaction rates depend on resonances widths (the imaginary part of the Siegert eigenvalues). As illustrated analytically for one-dimensional models and numerically for a more general random matrix version of Feshbach's optical model, transition state theory (TST, Rice–Ramsperger–Kassel–Marcus) provides the correct average unimolecular decay rate whether the resonances are overlapping or not. For all studied cases, the explicit "universal" dependence of the TST average rate on the average resonance width (for a given energy, or an energy interval) is that of a saturation curve: in the regime of nonoverlapping resonances (i.e., weak coupling) the standard relation "unimolecular decay rate=resonance width $/\hbar$" holds, but as the resonance overlap increases (strong coupling) the rate saturates, becoming practically independent of the average resonance width in the strong overlapping limit. On the basis of these conclusions, a discussion of what has been or can be measured in experiments of unimolecular decay that relates to the average decay rate and to the resonance widths is given. © *1994 American Institute of Physics.*

I. INTRODUCTION

The microscopic definition of the decay rate in unimolecular reactions is a central issue. However, it is more difficult to provide a rigorous theoretical definition of a unimolecular reaction rate than it is for a bimolecular reaction because there is in general no unambiguous way for separating the preparation of the initial (metastable) state of the molecule from its unimolecular decay. The exception to this confusing state of affairs is when the lifetime (inverse of the unimolecular decay rate) is extremely long, i.e., when the coupling between the metastable bound molecular state and the continuum to which it is coupled is weak. In this limit the rigorous description of the molecular system and its unimolecular decay is that of isolated (or nonoverlapping) resonances: the resonance states are characterized by complex energies, $\{E_n - i\Gamma_n/2\}$, which are the eigenvalues of the time-independent Schrödinger equation with outgoing wave boundary conditions (Siegert eigenvalues).[1(a)] The real part of an eigenvalue, E_n, is the energy of a particular metastable state, and the corresponding decay rate is given by its imaginary part (or width)

$$k_n = \frac{\Gamma_n}{\hbar}. \tag{1.1}$$

The requirement that the resonances be nonoverlapping is that the average width $\langle\Gamma\rangle$ is less than the average energy spacing ΔE,

$$\frac{\langle\Gamma\rangle}{\Delta E} < 1, \tag{1.2}$$

where the averages are over the set of metastable states in some relatively narrow energy region.

In most practical situations, however, unimolecular reactions do not correspond to this nonoverlapping regime. For example, for a typical rate $k \approx 10^{11}$ s^{-1}, Eq. (1.1) implies a width of $\Gamma \approx 0.5$ cm^{-1}, so that with a typical density of strongly mixed states $\rho \equiv 1/\Delta E$ that is many states per cm^{-1}, one has

$$\frac{\langle\Gamma\rangle}{\Delta E} \equiv \langle\Gamma\rangle\rho \gg 1, \tag{1.3}$$

the opposite to the nonoverlapping condition of Eq. (1.2). Siegert eigenvalues still exist in this overlapping situation, but in this case the unimolecular decay rate is not related to their widths in such a simple way as Eq. (1.1).[2] The primary purpose of this paper is to explore the relationship between rates and widths in the overlapping regime. Establishing this relationship in the regime of overlapping resonances has become particularly important, for it is now possible to carry out state-to-state studies of unimolecular reactions with initial state selection and measure both the reaction rates and spectral line shapes in the regime of overlapping resonances.[3–5] For small molecules that dissociate on a subpicosecond time scale, it is often easier to obtain linewidths than to carry out time-resolved measurements, and thus a clear understanding of the meaning of these two observables is important.

The standard RRKM approximation for unimolecular decay rates is based on microcanonical transition state theory (TST).[6,7] It is assumed that the metastable states of the reactant molecule are strongly mixed (ergodic) and that the usual transition state assumption of "direct dynamics" (or, in the language of classical mechanics, no recrossing trajectories) through the transition state bottleneck (local minimum of

[a]Permanent address: Department of Chemistry, University of Southern California, Los Angeles, CA 90089-0482.

 0021-9606/94/101(11)/9672/9/$6.00

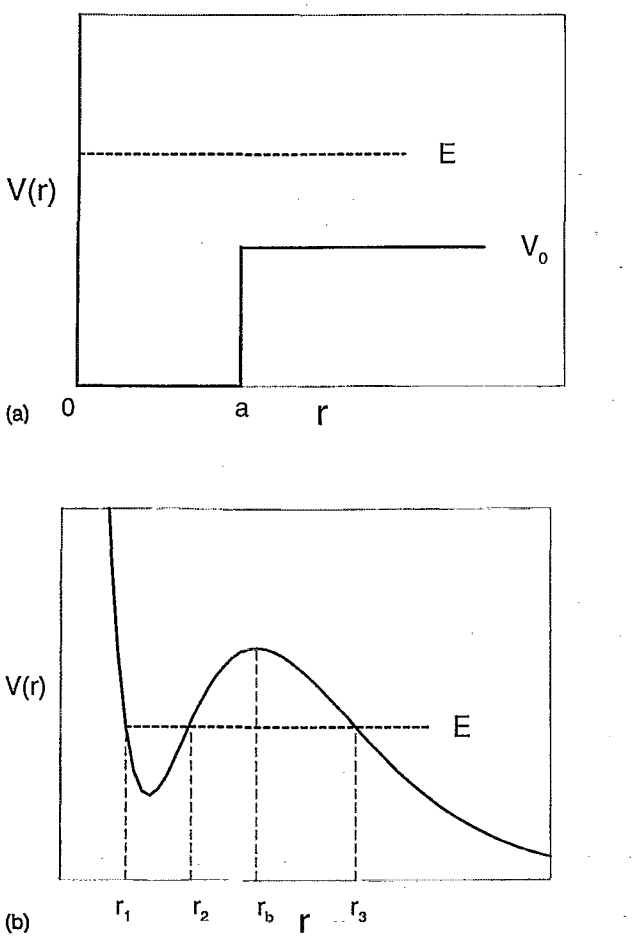

FIG. 1. (a) A square well potential. (b) A typical one-dimensional potential with a barrier.

flux through the TST dividing surface) is valid. The classical TST expression for the average rate for total energy E is

$$k_{\mathrm{TST}}(E)=\frac{N(E)}{2\pi\hbar\rho(E)}, \tag{1.4}$$

where the density of states, $\rho(E)$, is the number of reactant states per unit energy and $N(E)$ is the number of energetically accessible states of the activated complex (the molecule with the reaction coordinate degree of freedom removed) at the transition state dividing surface,[6]

$$N(E)=\sum_{\mathbf{n}^{\ddagger}} h(E-V_0-\epsilon_{\mathbf{n}^{\ddagger}}). \tag{1.5}$$

Here $h(\zeta)$ is the usual Heaviside function ($h=1$ for positive arguments, and $h=0$ otherwise), V_0 is the potential energy along the reaction coordinate at the transition state (the barrier height), and the energy levels of the activated complex are often approximated as harmonic oscillators

$$\epsilon_{\mathbf{n}^{\ddagger}}=\sum_{k=1}^{F-1} \hbar\omega_k^{\ddagger}(n_k^{\ddagger}+1/2), \tag{1.6}$$

where F is the number of vibrational degrees of freedom of the molecule and $\{\omega_k^{\ddagger}\}$ are the vibrational frequencies of the activated complex.[8] For total energies below the zero point energy corrected barrier height, i.e., $E < V_0 + \sum_{k=1}^{F-1} \frac{1}{2}\hbar\omega_k^{\ddagger}$, the classical TST rate is zero, so it is important to include tunneling corrections in this regime. The simplest one-dimensional tunneling correction generalizes Eq. (1.5) to[9]

$$N(E)=\sum_{\mathbf{n}^{\ddagger}} P_{\mathrm{1D}}(E-\epsilon_{\mathbf{n}^{\ddagger}}), \tag{1.7}$$

where $P_{\mathrm{1D}}(E_F)$ is the one-dimensional tunneling (or transmission) probability as a function of the energy available in the reaction coordinate, $E_F = E - \epsilon_{\mathbf{n}^{\ddagger}}$. More sophisticated approaches for determining $N(E)$, the cumulative reaction probability, are also possible, e.g., a nonseparable semiclassical version of TST,[10] and a fully rigorous quantum mechanical theory,[11,12] but the essential points to be established in this paper can be achieved by considering the simplest approximation for $N(E)$ [Eqs. (1.5) and (1.7)].

The major thesis and conclusion of the present paper is that the physically correct average unimolecular decay rate is well described by the TST rate whether the resonances are overlapping or not. In the nonoverlapping regime (i.e., isolated resonances) the rate is related to the widths of the Siegert eigenvalues in the usual way, Eq. (1.1). In the overlapping regime, however, the physically relevant unimolecular reaction rate is *not* related to the resonance widths by Eq. (1.1), though it is still well approximated by the TST rate. As the overlap increases, the TST rate becomes independent on the average width (saturates), which implies that in practice one cannot relate the average width to the TST rate in any simple way, and also that calculations of resonance widths alone are not capable of describing unimolecular reaction rates. This conclusion is supported by analysis of one-dimensional model problems and also by numerical simulations of a random matrix version of the Feshbach optical model of resonance states.

The plan of the paper is first to illustrate the situation with two simple one-dimensional examples in Sec. II, and then to treat the random matrix optical model in Sec. III. We conclude by commenting on the relation of the average width and rate to recent experimental measurements. The behavior seen in all cases is that

$$k_{\mathrm{TST}}(E)\leqslant\frac{\Gamma(E)}{\hbar}, \tag{1.8}$$

i.e., the average unimolecular decay rate is always less than or equal to the average width ($/\hbar$), equality maintaining in the low energy/nonoverlapping regime and the inequality becoming progressively more pronounced in the overlapping regime.

Finally, though the present paper deals primarily with the average unimolecular rate for a given total energy (or energy region), we note that TST has recently been combined with a random matrix description of the decaying system to provide a theory for the probability distribution of state specific decay rates in the nonoverlapping regime.[13] A similar description of the probability distribution of rates and widths can also be carried out for the overlapping regime. We show (*end*

of Sec. III) that a broad distribution of rates around the TST average [associated with a small $N(E)$] causes deviations of the effective decay rate from the TST value.

II. ONE-DIMENSIONAL MODELS

The general relation between rates and widths is correctly illustrated by one-dimensional systems, so it is useful to consider this simplest situation before proceeding to the more general model in Sec. III. We first consider a simple analytically solvable model, the square well potential, and then a general realistic potential within the WKB approximation.

A. Square well potential

For the square well potential, pictured in Fig. 1(a)

$$V(r)=\begin{cases}\infty, & r<0\\ 0, & 0<r<a\\ V_0, & r>a\end{cases} \tag{2.1}$$

one seeks solutions of the time-independent Schrödinger equation that are regular at the origin and have outgoing wave boundary conditions for $r>a$. The relevant wave functions are

$$\psi(r)=\text{const}\times\sin(kr),\qquad k=\sqrt{2mE/\hbar^2} \tag{2.2a}$$

for $0<r<a$, and

$$\psi(r)=\text{const}\times e^{iKr},\qquad K=\sqrt{2m(E-V_0)/\hbar^2} \tag{2.2b}$$

for $r>a$. Matching the logarithmic derivatives at $r=a$ in the usual fashion gives the following eigenvalue equation:

$$\cot(ka)=i\sqrt{1-\frac{V_0}{E}}, \tag{2.3}$$

which can be written in the following equivalent but more useful form:

$$k=(n+\tfrac{1}{2})\frac{\pi}{a}-\frac{i}{2a}\ln\left(\frac{1+\sqrt{1-V_0/E}}{1-\sqrt{1-V_0/E}}\right). \tag{2.4}$$

The Siegert eigenvalues are the complex roots of Eq. (2.4). It is easy enough to find these roots $\{E_n-i\Gamma_n/2\}$ numerically, but they are well approximated over the entire energy region $E>V_0$ by the following analytic expression:

$$E_n=\frac{\hbar^2\pi^2(n+1/2)^2}{2ma^2}, \tag{2.5a}$$

$$\Gamma_n=\frac{1}{2\pi}\frac{dE_n}{dn}\,2\ln\left(\frac{1+\sqrt{1-V_0/E_n}}{1-\sqrt{1-V_0/E_n}}\right). \tag{2.5b}$$

It is also useful to recall the transmission probability $P(E)$ for a particle passing over a step potential (i.e., at $r=a$)[14]

$$P(E)=1-\left(\frac{1-\sqrt{1-V_0/E}}{1+\sqrt{1-V_0/E}}\right)^2, \tag{2.6}$$

so that the width in Eq. (2.5b) can be written in terms of the transmission probability as

$$\Gamma_n=\frac{1}{2\pi}\frac{dE_n}{dn}\ln\left(\frac{1}{1-P(E_n)}\right). \tag{2.7}$$

The first factor in Eq. (2.7), $(1/2\pi)dE_n/dn$, when divided by $\hbar$, is the classical frequency of oscillation in the well; it is also related to the level spacing and density of resonance states,

$$\frac{dE_n}{dn}\equiv\Delta E=\frac{1}{\rho}. \tag{2.8}$$

For small transmission probabilities, $P(E_n)\ll 1$, i.e., energies E_n only slightly above V_0, one has $\ln[1-P(E_n)]^{-1}\approx P(E_n)$, so that from Eq. (2.7) one obtains

$$\lim_{E_n\to V_0}\Gamma_n=\frac{1}{2\pi}\frac{dE_n}{dn}P(E_n)=\frac{1}{2\pi\rho}P(E_n), \tag{2.9}$$

which is identical (when divided by $\hbar$) to the TST result for the one-dimensional rate [Eqs. (1.4) and (1.7)]

$$K_{\text{TST}}(E_n)=\frac{1}{2\pi\hbar}\frac{dE_n}{dn}P(E_n)=\frac{1}{2\pi\hbar\rho}P(E_n). \tag{2.10}$$

Note, however, that the TST rate, Eq. (2.10), is the correct rate for all values of P ($P\ll 1$ or $P\to 1$); i.e., the physically correct decay rate is the frequency of oscillation in the well multiplied by the escape probability per oscillation. Therefore, $\Gamma_n/\hbar$ is the physically correct rate only for $P\ll 1$. As $P\to 1$, i.e., in the high energy limit, Eqs. (2.6) and (2.7) give

$$\lim_{E_n\to\infty}\Gamma_n=\frac{1}{2\pi\rho}\ln(4E/V_0)^2 \tag{2.11a}$$

which is increasingly larger than the correct rate,

$$\lim_{E_n\to\infty}k_{\text{TST}}(E_n)=\lim_{P(E_n)\to 1}k_{\text{TST}}(E_n)=\frac{1}{2\pi\hbar\rho}, \tag{2.11b}$$

as the energy increases.

Since

$$P<\ln\left(\frac{1}{1-P}\right) \tag{2.12}$$

for all values of P, from Eqs. (2.7) and (2.10) one sees that

$$\frac{\Gamma_n}{\hbar}\geq k_{\text{TST}}(E_n), \tag{2.13}$$

with equality being approached in the lower energy/nonoverlapping regime, and the inequality becomes stronger at the higher energy/overlapping limit. Using Eqs. (2.7), (2.8), and (2.10), one can express the TST rate in terms of Γ_n

$$k_{\text{TST}}(E_n)=\frac{1}{2\pi\hbar\rho}(1-e^{-2\pi\rho\Gamma_n}) \tag{2.14}$$

which reveals quite clearly the characteristic features of the overlapping and non overlapping regimes,

$$k_{\text{TST}}(E_n)\approx\frac{\Gamma_n}{\hbar}\quad\text{for }\Gamma_n\rho\ll 1$$

and

$$k_{\mathrm{TST}}(E_n)\approx(2\pi\hbar\rho)^{-1} \quad \text{for } \Gamma_n\rho\gg 1.$$

The transition between the two regimes, i.e., $\Gamma_n\rho=1$, occurs when [see Eq. (2.10)]

$$P(E_n)=(1-e^{-2\pi})=0.998. \tag{2.15}$$

With P given by Eq. (2.6) for the present square well example, this corresponds to

$$E=V_0\cosh^2(\pi/2)\approx 6.3V_0, \tag{2.16}$$

i.e., an energy about 6 times the well depth.

B. Smooth potential barrier

Figure 1(b) shows a more realistic one-dimensional potential that is characteristic of a unimolecular decay process. Although one cannot obtain an exact analytic solution for a general potential, one can treat the general case within the WKB approximation (which is typically quite accurate for molecular systems).[15]

The WKB version of the Siegert eigenvalue condition is[16]

$$\Phi(E)=(n+1/2)\pi-\frac{i}{4}\ln(1+e^{-2\theta(E)}), \tag{2.17}$$

where $\Phi(E)$ is the phase integral across the well

$$\Phi(E)=\int_{r_1}^{r_2}dr\sqrt{2m[E-V(r)]/\hbar^2}, \tag{2.18a}$$

and $\theta(E)$ that through the barrier

$$\theta(E)=\int_{r_2}^{r_3}dr\sqrt{2m[V(r)-E]/\hbar^2}. \tag{2.18b}$$

For energies E above the barrier, $\Phi(E)$ is the phase integral from the repulsive wall to r_b (the top of the barrier) and $\theta(E)$—that between the two complex turning points that are the analytic continuations of r_2 and r_3. Again, one could find the complex roots of Eq. (2.17) numerically, but they are approximated well quite generally by expanding $\Phi(E)$ about the real part of the eigenvalue. The latter is then determined by the equation

$$\Phi(E_n)=(n+1/2)\pi, \tag{2.19}$$

the standard Bohr–Sommerfeld quantization condition for the well, and the width (imaginary part of the eigenvalue) is given by

$$\Gamma_n=\frac{1}{2\pi}\frac{dE_n}{dn}\ln(1+e^{-2\theta(E_n)}). \tag{2.20}$$

For energies not too high above the barrier, $\theta(E)$ is well described by the parabolic approximation,

$$\theta(E)=\frac{\pi}{\hbar\omega_b}(V_0-E), \tag{2.21}$$

where V_0 is the barrier maximum and ω_b its (real) harmonic frequency.

Recalling that the WKB transmission (or tunneling) probability through the barrier is[1(b)]

$$P(E)=\frac{1}{1+e^{2\theta(E)}}, \tag{2.22}$$

the width in Eq. (2.20) can also be expressed as

$$\Gamma_n=\frac{1}{2\pi}\frac{dE_n}{dn}\ln\left(\frac{1}{1-P(E_n)}\right), \tag{2.23}$$

precisely the same expression found above for the square well [Eq. (2.7)]. Thus essentially all of the above discussion for the square well potential also applies to the present more realistic (and general) potential, e.g., the TST rate is the frequency of oscillation inside the well multiplied by the escape probability per oscillation, according to Eq. (2.10). As before, the resonance width (when divided by $\hbar$) gives the rate correctly in the lower energy/tunneling/nonoverlapping regime, but is larger than the rate in the high energy/overlapping regime. The transition between these two regimes ($\Gamma_n\rho=1$) in the present case corresponds to $\ln(1+e^{-2\theta(E_n)})=2\pi$ [see Eq. (2.20)], or

$$\theta(E_n)=-1/2\ \ln(e^{2\pi}-1)\approx-\pi \tag{2.24}$$

which for the parabolic barrier [Eq. (2.21)] gives

$$E_n=V_0+\hbar\omega_b. \tag{2.25}$$

In other words, the overlapping regime is reached by the time the energy is approximately one vibrational quantum of the barrier frequency above the barrier.

Finally, one can use the results of this section to treat a general multidimensional system within the framework of the usual TST microcanonical convolution, i.e., the TST rate expression [Eqs. (1.4) and (1.7)],

$$k_{\mathrm{TST}}(E)=\frac{1}{2\pi\hbar\rho(E)}\sum_{\mathbf{n}^\ddagger}P_{1\mathrm{D}}(E-\epsilon_{\mathbf{n}^\ddagger}), \tag{2.26}$$

is a microcanonical average of the one-dimensional rate in Eq. (2.10).[17] Carrying out this same microcanonical average of the one-dimensional width expression, Eq. (2.7), one obtains the microcanonical average width (i.e., for total energy E) as

$$\Gamma(E)=\frac{1}{2\pi\rho(E)}\sum_{\mathbf{n}^\ddagger}\ln\left(\frac{1}{1-P_{1\mathrm{D}}(E-\epsilon_{\mathbf{n}^\ddagger})}\right). \tag{2.27}$$

In light of the inequality in Eq. (2.12) for any specific one-dimensional tunneling probability, one has the relation

$$k_{\mathrm{TST}}(E)\leqslant\Gamma(E)/\hbar$$

for all E, equality maintaining in the low energy/nonoverlapping regime. In the high energy limit one can obtain an approximate relation between $k_{\mathrm{TST}}(E)$ and $\Gamma(E)$ by going to the classical limit: neglecting tunneling [i.e., $P_{1\mathrm{D}}(E-\epsilon_{\mathbf{n}^\ddagger})\to h(E-V_0-\epsilon_{\mathbf{n}^\ddagger})$], using the harmonic approximation, and replacing the sums over $\mathbf{n}^\ddagger$ by integrals gives the classical RRK result for the TST rate,[6]

$$k_{\mathrm{TST}}^{\mathrm{cl}}(E)=\frac{1}{2\pi\hbar\rho(E)}\frac{(E-V_0)^{F-1}}{(F-1)!}\prod_{k=1}^{F-1}\frac{1}{\hbar\omega_k^\ddagger}. \tag{2.28}$$

In the expression for the microcanonical width, Eq. (2.27), one cannot simply replace $P_{1\mathrm{D}}$ by 0 or 1. However, for en-

ergies that are sufficiently low such that the parabolic approximation holds [Eqs. (2.21) and (2.22)], and yet are sufficiently high such that $|\theta(E)| \gg 1$, one has

$$\ln\left(\frac{1}{1-P_{1D}}\right)=\ln(1+e^{2|\theta(E)|})\approx\frac{2\pi}{\hbar\omega_b}(E-\epsilon_{n^\ddagger}-V_0). \tag{2.29}$$

Using this approximation in Eq. (2.27), and the other classical approximations noted above, one obtains

$$\Gamma^{cl}(E)=\frac{1}{\rho(E)\hbar\omega_b}\frac{(E-V_0)^F}{F!}\prod_{k=1}^{F-1}\frac{1}{\hbar\omega_k^\ddagger}. \tag{2.30}$$

Equations (2.28) and (2.30) thus give the following relation between $k_{TST}^{cl}(E)$ and $\Gamma^{cl}(E)/\hbar$:

$$\frac{\Gamma^{cl}(E)}{\hbar k_{TST}^{cl}(E)}=\frac{2\pi(E-V_0)}{\hbar\omega_b F} \tag{2.31}$$

which is valid in the high energy limit. As before, $\Gamma^{cl}(E)/\hbar$ becomes progressively larger than $k_{TST}^{cl}(E)$ as the energy increases.

From Eq. (2.30) for $\Gamma(E)$ one can also estimate the energy at which the transition between nonoverlapping and overlapping resonances takes place (on the average), i.e., when $\Gamma^{cl}(E)\rho=1$,

$$E=V_0+[(F!)\hbar\omega_b\Pi_{k=1}^{F-1}\hbar\omega_k^\ddagger]^{1/F}=V_0+(F!)^{1/F}\hbar\bar{\omega}^\ddagger, \tag{2.32}$$

where $\bar{\omega}^\ddagger$ is the geometric average of the transition state frequencies [including the (real) barrier frequency]. The transition to overlapping resonances therefore occurs at an energy of $\approx(F!)^{1/F}$ times $\hbar\bar{\omega}^\ddagger$ above the barrier, e.g., $(F!)^{1/F}\approx 2,\ 3,\ 4$, for $F=3,\ 6,\ 9$, respectively, and $(F!)^{1/F}\to F/e$ as $F\to\infty$.

III. RANDOM MATRIX OPTICAL MODEL

A popular and useful description of metastable states is the optical model, which is characterized by an effective non-Hermitian Hamiltonian. The formal derivation of the optical model Hamiltonian is based on the Feshbach/Löwdin partitioning of Hilbert space:[18,19] the projector Q is defined by a set of basis functions which span the bound state space of the molecule, and its complement, $P\equiv 1-Q$, projects onto the dissociative continuum to which it is coupled and decays. The effective Hamiltonian (which is a Q-space operator) is given by

$$\hat{H}_{eff}=QHQ+\lim_{\epsilon\to 0}QHP(E+i\epsilon-PHP)^{-1}PHQ\equiv\hat{H}_0-\frac{i}{2}\hat{\Gamma}, \tag{3.1a}$$

where

$$\hat{\Gamma}=2\pi QHP\delta(E-PHP)PHQ. \tag{3.1b}$$

In most applications of the optical model[13,19–22] the width operator $\hat{\Gamma}$ is taken to be energy independent, which is not a severe approximation if one considers a group of molecular bound states all in a relatively narrow energy regime. The operators $\hat{H}_0$ and $\hat{\Gamma}$ in Eq. (3.1) are both Hermitian, so $\hat{H}_{eff}$ is not; it describes the metastable Q space. If $\psi(0)$ is the initial Q-space state, then its Q-space component at time t later is

$$|\psi(t)\rangle=e^{-i\hat{H}_{eff}t/\hbar}|\psi(0)\rangle, \tag{3.2}$$

and its effective decay rate is defined as the logarithmic derivative of its norm,

$$k_{eff}(t)\equiv-\frac{d}{dt}\ln\langle\psi(t)|\psi(t)\rangle. \tag{3.3}$$

The eigenvalues of $\hat{H}_{eff}$ are complex, $\{E_l-i\Gamma_l/2\}$, the counterpart to the Siegert eigenvalues discussed in Sec. II. If the initial state $|\psi(0)\rangle$ has nonzero overlap with only one of the eigenstates of $\hat{H}_{eff}$, then

$$|\psi(t)\rangle=e^{-i(E_l-i\Gamma_l/2)t/\hbar}|\psi(0)\rangle, \tag{3.4a}$$

and the rate defined by Eq. (3.3) is simply

$$k_{eff}(t)=\frac{\Gamma_l}{\hbar}, \tag{3.4b}$$

the standard relation for an isolated resonance. In the more general case, however, the resonance states overlap, and the initial state will typically overlap more than one state. The decay rate in this case will not be related to the resonance widths in a simple fashion. Rather, it is necessary to determine the decay rate directly from Eqs. (3.2) and (3.3).

To carry out calculations of the unimolecular rate, we adopt a random matrix version of the optical model, similar to that used by other authors.[13,20–22] The (Q space) matrix representation of $\hat{H}_{eff}$ is

$$H_{m,m'}^{eff}=E_m\delta_{m,m'}-i\pi\sum_{n=1}^{N}V_{n,m}V_{n,m'}, \tag{3.5}$$

$m,m'=1,\ldots,M$. We assume that the molecular states are strongly mixed (ergodic), so the energies E_m are chosen from a Wigner distribution of nearest-neighbor level spacings,

$$f(S_m)=\frac{\pi S_m}{2\langle S_m\rangle^2}\exp\left(-\frac{\pi S_m^2}{4\langle S_m\rangle^2}\right), \tag{3.6a}$$

where $S_m=E_m-E_{m-1}$, and the average spacing is determined by the density of molecular states, ρ,

$$\langle S_m\rangle\equiv\Delta E=\frac{1}{\rho}. \tag{3.6b}$$

The average bandwidth in energy space of the M molecular states is therefore $W=\rho M$. The width matrix in Eq. (3.5), i.e.,

$$\Gamma_{m,m'}=2\pi\sum_{n=1}^{N}V_{n,m}V_{n,m'}, \tag{3.7}$$

describes the coupling of the M states in the Q space to N independent decay channels in the P space. The $Q-P$ coupling matrix elements, $V_{n,m}$, are chosen randomly from a Gaussian (normal) distribution with mean value 0 and standard deviation σ; thus

$$\langle V_{n,m}V_{n',m'}\rangle=\delta_{n,n'}\delta_{m,m'}\sigma^2. \tag{3.8}$$

For a given realization of the effective Hamiltonian (i.e., a given random selection of the matrix elements as discussed above), its eigenvalues $\{E_l - i\Gamma_l/2\}$ are obtained by diagonalizing the matrix numerically. The average width of all M eigenstates,

$$\bar{\Gamma} = \frac{1}{M} \sum_{l=1}^{M} \Gamma_l \tag{3.9a}$$

is determined by the sum rule

$$\bar{\Gamma} = \frac{1}{M} \operatorname{tr} \Gamma = \frac{2\pi}{M} \sum_{m=1}^{M} \sum_{n=1}^{N} V_{n,m}^2, \tag{3.9b}$$

and the average of $\bar{\Gamma}$ over the random matrix ensemble (i.e., the distribution of coupling matrix elements, $V_{n,m}$) gives [see Eq. (3.8)],

$$\langle \bar{\Gamma} \rangle = 2\pi\sigma^2 N. \tag{3.10}$$

In the nonoverlapping regime, $\langle \bar{\Gamma} \rangle \rho \ll 1$, the average unimolecular decay rate is expected to be related to the average resonance width in the usual way,

$$k_{\text{eff}}(t) \approx \bar{\Gamma}/\hbar \tag{3.11}$$

and indeed this is found in our numerical simulations [see Fig. 2(a)]. By expanding the norm in powers of t and keeping only the linear term, it can readily be shown that the short time decay rate is always given by the average resonance width divided by $\hbar$, i.e.,

$$\lim_{t \to 0} k_{\text{eff}}(t) = \frac{\bar{\Gamma}}{\hbar}. \tag{3.12}$$

However, when the resonances overlap, the time interval over which Eq. (3.12) holds becomes too short to be significant, as illustrated in Fig. 2(b). We have taken the operational definition of the time-independent rate, k_{eff}, to be the best exponential fit to the decay of the norm over the time interval for which it is diminished by two orders of magnitude (i.e., from 1 to $\approx 10^{-2}$). In the nonoverlapping regime, Eq. (3.12) holds for sufficiently long time to describe the entire decay process, but in the overlapping regime, it corresponds merely to an insignificant initial transient.

In Fig. 3, the decay rates, k_{eff}, obtained as described above, are plotted as a function of the average resonance width $\langle \bar{\Gamma} \rangle$, for fixed values of the density of states, ρ, and the number of open channels, N. For sufficiently small $\langle \bar{\Gamma} \rangle$, (the nonoverlapping regime), a linear dependence is observed according to Eq. (3.11) with a slope of 1 as $\langle \bar{\Gamma} \rangle \to 0$. As $\langle \bar{\Gamma} \rangle$ increases into the overlapping regime, deviations from the linear dependence are observed, until saturation of the curves is reached, indicating an increasingly larger difference between the decay rate ($\times \hbar$) and the average resonance width.

The saturation phenomenon can be understood physically by invoking a "kinetic picture" of the optical model. When the average coupling strength is much smaller than the average level spacing in the molecular complex, i.e., $\sigma^2\rho \to 0$ (the nonoverlapping regime), the "rate limiting step" in the decay is the transition from specific states in Q to specific states in P (the state-to-state transition probabilities in the "golden rule" limit). As $\sigma^2\rho$ increases (the overlapping regime), the state-to-state rate become large and the total decay rate is limited only by the "volumes" of the spaces Q and P, i.e., the number of molecular states per energy, ρ, and the number of independent open channels, N. Therefore, for fixed values of ρ and N, the rate depends on the coupling strength in the nonoverlapping regime, but saturates as a function of σ^2 in the overlapping regime.

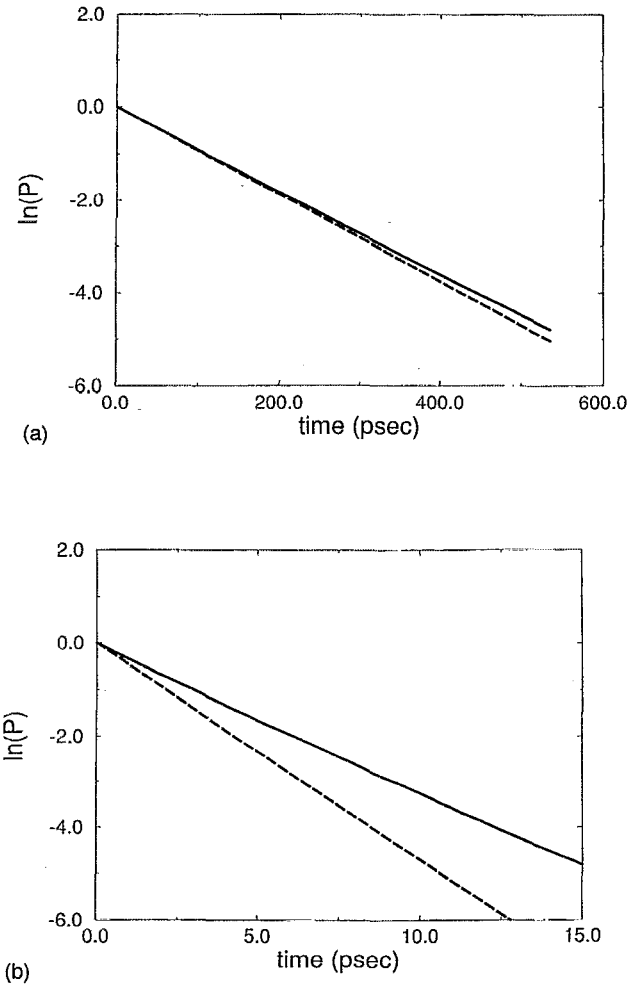

FIG. 2. (a) Solid line: A typical simulation of a unimolecular decay in the regime of non-overlapping resonances ($\bar{\Gamma}\rho = 0.25$). The solid line corresponds to the actual decay of a normalized random initial state, $P = \langle \psi(t) | \psi(t) \rangle$, for an effective Hamiltonian with $N = 100$, $M = 800$, and $\rho = 5$ states per wave number. The dashed line corresponds to the average resonance decay rate, $P = \exp(-\bar{\Gamma}t/\hbar)$. (b) The same for overlapping resonances ($\bar{\Gamma}\rho = 12.5$).

A more quantitative physical understanding of this saturation phenomenon can be obtained from the correspondence between the present random matrix optical model and the TST picture discussed in Sec. II B. To this end we write the average width in Eq. (3.9b) as

$$\bar{\Gamma} = \sum_{n=1}^{N} \gamma_n, \tag{3.13a}$$

where

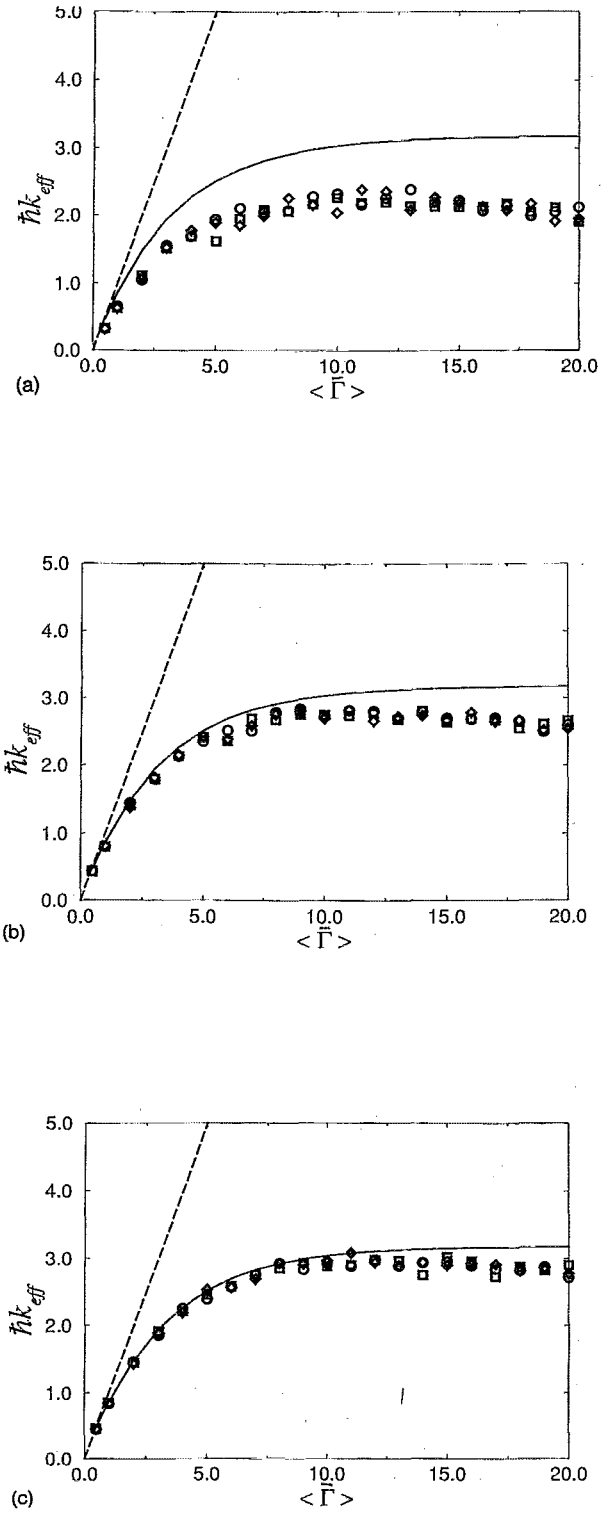

FIG. 3. (a) Decay rates for a random initial state, plotted as a function of the average resonance widths (in wave numbers). The different symbols correspond to different random choices of the effective Hamiltonian matrix with $N=10$ and $\rho=0.5$ states per wave number. $M=600$ was found large enough to provide a reliable statistical ensemble. The solid line is the TST result for the ensemble average [Eq. (3.16a)], and the dashed line is the result of equating the averaged rate ($\times\hbar$) to the averaged resonance width. (b) The same, with $N=50$ and $\rho=2.5$ states per wave numbers. (c) The same, with $N=100$ and $\rho=5$ states per wave number.

$$\gamma_n=\frac{2\pi}{M}\sum_{m=1}^{M}V_{n,m}^2, \tag{3.13b}$$

and interpret γ_n as the average width of channel n (the average partial width). Furthermore, we identify the independent final channels in the optical model with the states of the activated complex in TST, so that by equating the average width in Eq. (3.13a) with the microcanonically averaged width given by TST, Eq. (2.27), we obtain

$$\gamma_n=\frac{1}{2\pi\rho}\ln\left(\frac{1}{1-P_n}\right), \tag{3.14a}$$

or

$$P_n=1-e^{-\gamma_n 2\pi\rho}. \tag{3.14b}$$

Making use of Eq. (3.14b) for the transmission probability, the average TST rate is obtained from Eq. (2.26)

$$\bar{k}_{\mathrm{TST}}=\frac{1}{2\pi\hbar\rho}\sum_{n}(1-e^{-2\pi\gamma_n\rho}) \tag{3.15a}$$

or by using Eq. (3.13b) for γ_n

$$\bar{k}_{\mathrm{TST}}=\frac{1}{2\pi\hbar\rho}\sum_{n}\left[1-\exp\left(-\frac{4\pi^2\rho}{M}\sum_{m=1}^{M}V_{n,m}^2\right)\right]. \tag{3.15b}$$

Averaging Eq. (3.15b) over the random matrix ensemble finally gives

$$\langle\bar{k}_{\mathrm{TST}}\rangle=\frac{N}{2\pi\hbar\rho}\left[1-\left(1+\frac{4\pi\rho\langle\bar{\Gamma}\rangle}{NM}\right)^{-M/2}\right], \tag{3.16a}$$

which in the limit $M\to\infty$ becomes

$$\lim_{M\to\infty}\langle\bar{k}_{\mathrm{TST}}\rangle=\frac{N}{2\pi\hbar\rho}(1-e^{-2\pi\langle\bar{\Gamma}\rangle\rho/N}). \tag{3.16b}$$

[Note that for $N=1$, Eq. (3.16b) is the same as the one-dimensional result of Sec. II, Eq. (2.14)!]

Equation (3.16) clearly shows that in the nonoverlapping limit,

$$\lim_{\langle\bar{\Gamma}\rangle\rho\to 0}\langle\bar{k}_{\mathrm{TST}}\rangle=\frac{\langle\bar{\Gamma}\rangle}{\hbar}, \tag{3.17a}$$

while the saturation behavior is apparent at large overlap

$$\lim_{\langle\bar{\Gamma}\rangle\rho\to\infty}\langle\bar{k}_{\mathrm{TST}}\rangle=\frac{N}{2\pi\hbar\rho}, \tag{3.17b}$$

where the latter limit has the "classical" TST form for the reaction rate. The solid lines in Fig. 3 are obtained by using Eq. (3.16a), and they are seen to provide a qualitatively correct description of the saturation phenomenon observed in the numerical simulations. This suggests that the above TST interpretation of the random matrix optical model is qualitatively correct. However, quantitative agreement between the simulated decay rates (i.e., k_{eff}) and the TST average rate is obtained only when N, the number of independent open channels, is large enough (see Fig. 3). This is most apparent in looking at the large $\langle\bar{\Gamma}\rangle$ "plateau" values of the rates,

where the simulated results (the points) fall below the TST values (the curve), the more so the smaller N. This, however, is not related to a failure of the TST interpretation, but rather to deviations of the actual (simulated) decay process from a single exponential. Deviations from a single exponential are associated with a distribution of state-specific rates about the average value. To show how this reduces the effective decay rate with respect to the averaged TST rate, we assume the well known χ^2 probability distribution[13,18,23] of rates about $\langle \bar{k}_{\mathrm{TST}} \rangle$,

$$P(k)=\left(\frac{N}{2\langle \bar{k}_{\mathrm{TST}} \rangle}\right)^{N/2} \frac{k^{N/2-1}}{\Gamma(N/2)}\, e^{-Nk/(2\langle \bar{k}_{\mathrm{TST}} \rangle)}, \tag{3.18}$$

where the distribution width is determined by N, the number of decay channels. The decay of the system is then given by[24]

$$\mathcal{N}(t)=\int_0^\infty dk P(k) e^{-kt}=\left(1+\frac{2\langle \bar{k}_{\mathrm{TST}} \rangle t}{N}\right)^{-N/2}, \tag{3.19a}$$

which in the limit of large N gives pure exponential decay,

$$\lim_{N\to\infty} \mathcal{N}(t)=e^{-\langle \bar{k}_{\mathrm{TST}} \rangle t}, \tag{3.19b}$$

where $\mathcal{N}(t)$ is the norm of an arbitrary state in the Q space, $\langle \psi(t)|\psi(t) \rangle$. The effective time-independent decay rate for a finite time interval, $0<t<T$, is the average of the time-dependent effective rate defined in Eq. (3.3),

$$k_{\mathrm{eff}}=\frac{1}{T}\int_0^T dt\left(-\frac{d}{dt}\ln(\mathcal{N}(t))\right)=\frac{-1}{T}\ln[\mathcal{N}(T)]. \tag{3.20}$$

By using Eq. (3.19) one obtains the following explicit relation between the effective decay rate and the TST average rate:

$$k_{\mathrm{eff}}=\langle \bar{k}_{\mathrm{TST}} \rangle \frac{2\ln[\mathcal{N}(T)]}{N\{1-[\mathcal{N}(T)]^{-2/N}\}}, \tag{3.21a}$$

and one can easily show that

$$\lim_{N\to\infty} k_{\mathrm{eff}}=\langle \bar{k}_{\mathrm{TST}} \rangle. \tag{3.21b}$$

Thus for infinite N the effective decay rate over any time interval is given by the TST average rate, but for finite N, k_{eff} is smaller than the TST rate, and their ratio depends on $\mathcal{N}(T)$. In the present simulations, the time interval T was defined such that $\mathcal{N}(T)\approx 10^{-2}$. According to Eq. (3.21a), for $N=10$, 50, and 100, this choice gives $k_{\mathrm{eff}}/\langle \bar{k}_{\mathrm{TST}} \rangle=0.60$, 0.91, 0.95, respectively, which is in a good agreement with the results in Fig. 3 (i.e., these ratios correspond to the deviations of the simulated effective rates from the TST curve).

Note that although the TST expression for the rate agrees well with the simulations, the correspondence between TST and the present optical model is not precise, because the parametrization in the two models is different. For example, according to TST the coupling of the molecular complex to the different decay channels (i.e., states of the activated complex) varies greatly depending on the energy available to the reaction coordinate, whereas in the random matrix model all decay channels are equivalent. Also, in TST an increase in the average coupling always corresponds to an increase in the number of decay channels [$N(E)$], while in the optical model they are independent parameters. One could, of course, refine the optical model, e.g., by adopting different average coupling strengths, $V^2_{n,m}$, for different channels n, and this might indeed be useful in applications to specific molecular systems.

Finally, we note in Fig. 3 that when the resonance overlap becomes sufficiently large, the average decay rate actually decreases as a function of $\langle \bar{\Gamma} \rangle=2\pi N\sigma^2$, in contradiction to the prediction of the TST model, Eq. (3.16), and to the physical interpretation of the optical model. Our simulations indicate that this behavior appears approximately when the degree of resonance overlap exceeds the number of decay channels, i.e., when

$$\rho\langle \bar{\Gamma} \rangle > N. \tag{3.22}$$

This condition is identical to the onset of a bifurcation in the distribution of resonance widths in the optical model, which has recently been discussed by several authors.[20,22] In our opinion this behavior signals the breakdown of the optical model itself and is not due to a failure of the TST interpretation of the rate, i.e., we argue that the results of the optical model become physically irrelevant once the condition (3.22) is met. The reasoning is as follows: The basis set in which the effective Hamiltonian matrix is represented covers a spectral energy range of $W=M/\rho$. This basis provides a reliable representation of the Hamiltonian only as long as its eigenvalues are confined to a circle in the complex energy plane with radius $W/2$. This limitation implies the restriction

$$\max(\Gamma_l) < W. \tag{3.23}$$

A rough estimate for the maximum resonance width can be obtained in the "reversed" perturbative limit, where the real part of the Hamiltonian matrix is negligible with respect to the imaginary part. The imaginary part is an $M\times M$ matrix of rank N. Therefore $M-N$ of its eigenvalues (widths) are zero (This is in fact the reason for the observed bifurcation). In this limit, a lower bound estimate for the largest width is given by the average of the N nonzero eigenvalues, $M\langle \bar{\Gamma} \rangle/N$. Using this estimate, the condition in Eq. (3.19) for the relevance of the optical model is $\langle \bar{\Gamma} \rangle M/N<W$, or $\langle \bar{\Gamma} \rangle \rho<N$, precisely the opposite of Eq. (3.22). We thus conclude that the phenomenon of bifurcation in the distribution of widths and the decrease of the decay rate with increasing average resonance width are associated with an improper sampling of the spectrum of H_{eff} within the finite representation of the Q space.

IV. CONCLUDING REMARKS

From several different points of view, including analytical treatments of simple one-dimensional systems and numerical simulations of a random matrix version of the optical model, we conclude that the TST (RRKM) rate constant gives the physically correct unimolecular reaction rate whether the complex (Siegert) eigenvalues which characterize the metastable molecular system are overlapping or not. In the limit that the resonances do not overlap, the standard relation $k=\Gamma/\hbar$ holds, but not so in the overlapping regime,

for which $k<\Gamma/\hbar$, the more so the greater the degree of overlap. Furthermore, we were able to give a transition state theory interpretation of the numerical simulations of the random matrix optical model which explains how the effective decay rate "saturates" as the coupling strength (degree of resonance overlap) increases.

In concluding, we briefly discuss what has been or can be measured in experiments of unimolecular decay that relates to the average decay rate and to the resonance widths. The average decay rate can, of course, be measured in time-resolved experiments, whether the resonances are overlapping or not. Averaging is inherent in measurements of fast decay rates, since the energy resolution is limited by the uncertainty relation between the pulse duration and its energy. Thus, the rates derived from such measurements can be compared directly to the TST/RRKM predictions. Note that as the number of states of the activated complex $[N(E)]$ decreases, the distribution of decay rates around the average value becomes broader, which implies that the measured (effective) decay rate may not correspond directly to the TST rate.

In contrast to the rates, the true resonance widths can be measured only in the regime of isolated resonances. Although the present work suggests a universal relation between the average TST rate and the averaged resonance width also in the overlapping regime, the saturation of the rate (at the classical RRKM value) as the resonance overlap increases, implies that in practice one cannot extract the resonance widths from measurements of rates in this regime, not even on the average.

In the regime of nonoverlapping resonances, one can measure the resonance widths directly. When the coupling to the continuum is relatively weak, the total absorption spectrum and the partial spectra into specific product channels will exhibit spectral features of Lorentzian shape, whose widths can be identified with the resonance widths (the imaginary part of the Siegert eigenvalues). In the regime of overlapping resonances, the observed spectral features are governed by superpositions (with complex coefficients) of overlapping resonance amplitudes. Therefore, in this regime the shapes of the spectral features are usually not Lorentzian and the resonance widths are not directly related to the experimental observables.

The interpretation of the observed spectral line shapes is an interesting subject for future research. Recent measurements of final state-selected spectra of NO_2 photodissociation[25] have indicated that the average spectral linewidth over a given energy range is not too different from the unimolecular decay rate ($\times\hbar$) obtained in time-resolved measurements,[5] even in the overlapping regime. We argue, however, that in general, in the overlapping regime, the observed linewidths are not related in a simple fashion either to the unimolecular decay rate or to the resonance widths.

Finally, we point out that fluctuations in the decay rates about the TST average have been demonstrated experimentally and treated theoretically in the case of isolated resonances.[13,21,23] The TST interpretation of the optical model can be used to characterize these fluctuations also in the regime of overlapping resonances. An indirect experimental observation, suggesting that such fluctuations do exist in the case of overlapping resonances, have been obtained recently[26] in the unimolecular decay of NO_2.

ACKNOWLEDGMENTS

H. R. would like to thank W. H. Miller and C. B. Moore for the hospitality during her Sabbatical stay at Berkeley, and U. P. thanks the Fulbright and the Rothschild foundations for postdoctoral fellowships. This work was supported by the Director, Office of Energy Research, Office of Basic Energy Sciences, Chemical Sciences Division of the U.S. Department of Energy under Contract Nos. DE-AC03-76SF00098 (to W. H. M.) and DE-FG03-88ER13959 (to H. R.).

[1] L. D. Landau and E. M. Lifshitz, *Quantum Mechanics* (Pergamon, London, 1958), (a) pp. 440–441; (b) pp. 177–178.
[2] T. Seideman and W. H. Miller, J. Chem. Phys. **95**, 1768 (1991).
[3] (a) S. A. Reid, J. T. Brandon, M. Hunter, and H. Reisler, J. Chem. Phys. **99**, 4860 (1993); (b) S. A. Reid, D. C. Robie, and H. Reisler, *ibid.* **100**, 4256 (1994); (c) S. A. Reid and H. Reisler, *ibid.* (in press).
[4] J. Miyawaki, K. Yamanouchi, and S. Tsuchiya, J. Chem. Phys. **99**, 254 (1993).
[5] (a) G. A. Brucker, S. I. Ionov, Y. Chen, and C. Wittig, Chem. Phys. Lett. **194**, 301 (1992); (b) S. I. Ionov, G. A. Brucker, C. Jaques, Y. Chen, and C. Wittig, J. Chem. Phys. **99**, 3420 (1993); (c) C. Wittig and S. I. Ionov, *ibid.* **100**, 4717 (1994).
[6] P. J. Robinson and K. A. Holbrook, *Unimolecular Reactions* (Wiley, New York, 1972).
[7] W. Forst, *Theory of Unimolecular Reactions* (Academic, New York, 1973).
[8] For simplicity, rotation is ignored in Eqs. (1.4)–(1.6), and a rigid TS is assumed. If there is no well defined barrier, then the TS must be determined variationally: $V_0 \rightarrow V_0(s)$, $\omega_k^{\ddagger} \rightarrow \omega_k^{\ddagger}(s)$ in Eqs. (1.5), (1.6), and the TS is chosen to be the value of the reaction coordinate, s, for which $N(E;s)$ is a minimum. These features are well understood and can be easily incorporated in all the treatment throughout the paper, but for simplicity of presentation they will not be indicated explicitly.
[9] R. A. Marcus, J. Chem. Phys. **45**, 2138 (1966); W. H. Miller, J. Am. Chem. Soc. **101**, 6810 (1979).
[10] W. H. Miller, R. Hernandez, N. C. Handy, D. Jayatilaka, and A. Willets, Chem. Phys. Lett. **172**, 62 (1990).
[11] W. H. Miller, J. Chem. Phys. **62**, 1899 (1975); W. H. Miller, S. D. Schwartz, and J. W. Tromp, *ibid.* **79**, 4889 (1983); T. Seideman and W. H. Miller, *ibid.* **96**, 4412 (1992), U. Manthe and W. H. Miller, *ibid.* **99**, 3411 (1993).
[12] N. Rom, V. Ryaboy, and N. Moiseyev, J. Chem. Phys. **98**, 6327 (1993); N. Rom and N. Moiseyev, *ibid.* **99**, 7703 (1993).
[13] W. F. Polik, C. B. Moore, and W. H. Miller, J. Chem. Phys. **89**, 3584 (1988); W. F. Polik, D. R. Guyer, C. B. Moore, and W. H. Miller, *ibid.* **92**, 3471 (1990); W. H. Miller, R. Hernandez, and C. B. Moore, *ibid.* **93**, 5657 (1990).
[14] A. Messiah, *Quantum Mechanics* (Wiley, New York, 1968).
[15] M. S. Child, *Semiclassical Mechanics with Molecular Applications* (Oxford University Press, New York, 1991).
[16] W. H. Miller, *Advances in Chemical Physics*, edited by K. P. Lawley (Wiley, New York, 1975), Vol. 30; B. A. Waite and W. H. Miller, J. Chem. Phys. **76**, 2412 (1982).
[17] W. H. Miller, Chem. Rev. **87**, 19 (1987).
[18] H. Feshbach, *Theoretical Nuclear Physics* (Wiley, New York, 1992).
[19] R. D. Levine, *Quantum Mechanics of Molecular Rate Processes* (Clarendon, Oxford, 1969).
[20] I. Rotter, Rep. Prog. Phys. **54**, 635 (1991); W. Iskra, I. Rotter, and F.-M. Dittes, Phys. Rev. C **47**, 1086 (1993).
[21] M. D.-Lecomte and F. Culot, J. Chem. Phys. **98**, 7819 (1993).
[22] K. Someda, H. Nakamura, and F. H. Mies, Chem. Phys. **187**, 195 (1994).
[23] R. D. Levine, Ber. Bunsenges. Phys. Chem. **92**, 222 (1988).
[24] W. H. Miller, J. Phys. Chem. **92**, 4261 (1988).
[25] S. A. Reid and H. Reisler (unpublished results).
[26] S. A. Reid and H. Reisler (to be published).